

Małgorzata Jastrzębska*, Marian Łupieżowiec

Application of Clay–rubber Mixtures for the Transportation Geotechnics—the Numerical Analysis

<https://doi.org/10.2478/sgem-2023-0020>

received February 1, 2023; accepted August 31, 2023.

Abstract: The use of waste materials (including rubber) in industry is one of the most important issues in terms of environmental protection. One of such applications is the use of soil–rubber mixtures in backfills or lower layers of embankments or road structures. The numerical analyses of the behavior of a clay–rubber mixture layer built into a road embankment are presented in this article. An elastic–perfectly plastic model with a Coulomb–Mohr yield surface was used in the finite element analysis. The parameters of soil–rubber mixtures adopted for the analysis were estimated on the basis of triaxial tests: monotonic (UU—unconsolidated undrained, and CU—consolidated undrained) and cyclic (CU) performed with low frequency ($f = 0,001$ Hz). The triaxial tests were carried out on mixtures of kaolin (K) and red clay (RC) with the addition of 1–5 mm rubber granulate (G) in the amount of 5–25% by weight. Numerical analyses included a static plate load test (VSS) of a layer made of a rubber–soil mixture built into the embankment and testing the stability of embankments using the c – ϕ strength reduction procedure. The results of laboratory tests confirm the necessity of testing soil–rubber mixtures each time before their use in embankments. The observed overall decrease in shear strength and stiffness of the tested material is variable and depends on the type of soil and the content of rubber waste. Satisfactory results of the analysis were obtained, both in terms of the values of layer stiffness modules and slope safety factors, which allows for the conclusion of the possibility of using soil–rubber mixtures (with the recommended granulate addition up to 30% by weight)

in the layers of road embankments and (depending on the road class) in the lower layers of the pavement structure.

Keywords: clay–rubber waste mixtures; cyclic loads; road layer stiffness; stability of road embankment; VSS load tests.

1 Introduction

With increasing environmental awareness, the idea of sustainable development has become widespread. It is very important to meet the human socioeconomic needs in the context of maintaining ecological balance. This task is also undertaken by geotechnical engineers, whose work focuses on three broad areas: sustainable improvement/reinforcement of weak subsoil, sustainable foundation design, and sustainable geotechnical design. These activities include, for example: (1) the use of alternative environmentally friendly materials in geotechnical constructions such as embankments, slopes, dams; (2) reuse of waste such as rubber tires, fly ash, natural or artificial fibers for improvement and stabilization; and (3) conscious design and modeling based on geotechnical parameters. For years, these issues have been widely discussed, analyzed, and practiced in geotechnical engineering [22,31,32,48,52], especially in transportation geotechnics [10,51]. Difficult and complicated geotechnical conditions are considered, e.g. when the subsoil contains weak cohesive soils of plastic consistency or shows volume changes (swelling or shrinking) under the influence of changes in water content [25]. In the case of such soils, actions are taken to reduce the weight of the embankments built on them or to reduce their swelling [27]. Rubber waste from car tires can be used for this purpose, according to the rule “end-of-life tires” (ELT). Each such new application requires research [18,24,50]. Among the tests performed, direct shear tests [6,28,45], unconfined compression tests or triaxial tests [1,18,46] dominate. The two basic conclusions presented in the available literature

*Corresponding author: Małgorzata Jastrzębska, Katedra Geotechniki i Dróg, Wydział Budownictwa, Politechnika Śląska, ul. Akademicka 5, 44-100 Gliwice, E-mail: malgorzata.jastrzebska@polsl.pl

Marian Łupieżowiec, Katedra Geotechniki i Dróg, Wydział Budownictwa, Politechnika Śląska, ul. Akademicka 5, 44-100 Gliwice

are: (1) regardless of the type of soil, its unit weight when added to rubber waste decreases and reduces the weight of the structure [16] and (2) the mechanical properties of soil–rubber mixtures vary depending on the type of soil, the type of waste rubber used (size/shape [42,43]), and its percentage (weight or volume; [9,46]).

An interesting research problem arises here, the aim of which is the practical use of cohesive soils–rubber waste mixtures in geoen지니어ing as light embankments on weak soils or for the construction of road or railway embankments. This issue finds its solution not only by experiment but also by design.

Nowadays, the basis of the design process is the performance of many numerical analyses that allow the simulation of future processes of impact on the designed object [4]. Based on the performed analyses, it is possible to prove the fulfillment of limit states, both ultimate and serviceability. They allow for the consideration of many cases and variants, which allows for the optimal selection of construction and material solutions to be able to erect a safe and functional facility. In particular, numerical analyses play an important role when using new materials, for which a number of laboratory tests have been carried out, but the application of which has not yet been tested in practical implementations [8].

The first problem is the need to obtain a suitable base for the construction of the road surface. According to polish standards, in road construction, properties in this area are checked in trial load tests with a rigid VSS steel plate [38]. On roads with a higher traffic load, it is required that the value of the secondary deformation modulus E_2 , which is a measure of the subsoil stiffness (in road jargon called load capacity), is not less than 120 MPa [39]. In addition, there is a restriction on the value of the deformation index $I_0 = E_2/E_1$ was not greater than 2.2. The fulfillment of the latter condition results in the reduction of plastic deformations to an acceptable level. Owing to this, ruts are not observed in the places where car wheels pass, which significantly increases the durability of the road surface. The second considered issue is the stability of road embankment slopes, which is important for embankments of greater height [49]. The slope inclination of 1:1.5, used as a standard in Polish road engineering, makes it necessary to perform stability analyses each time the height of a communication structure is greater than 3.0 m. The stability of slopes is greatly influenced by the strength properties of the material used to build the subject object. In engineering practice in Poland, it is required to obtain a value of the stability coefficient not lower than 1.5 [39], which means a very large safety margin. Usually, the requirements in the slope stability are clearly lower [49].

All the issues very important in the design of road embankments and pavement structures presented above were taken into account during the planning and implementation of triaxial tests and numerical analyses, and are discussed in the following sections.

2 Laboratory tests—materials used and test conditions

2.1 Fine-grained soils

Two cohesive soils from Southern Poland were selected for the tests. One of them of a characteristic red color (hence the usable name—red clay (RC) [29] came from Triassic deposits in Patoka, near Częstochowa. While the other soil, named by us—kaolin (K), came from the Porcelain Factory in Tułowice. According to a classification consistent with the standard PN-EN ISO 14688-2:2006 [34] and the unified soil classification system (USCS) [3], these are respectively:

- Swelling (RC)—clay with silt (siCl) [34]/clay with high plasticity (CH) [3]: $d_{10} = 0.0008$ mm, $d_{50} = 0.0045$ mm, $d_{90} = 0.02$ mm, $C_c = 0.63$, $C_u = 100$, $f_{cl} = 29\%$, $f_{si} = 71\%$, $PL = 25\%$, $LL = 75\%$, $\sigma_{sp} = 97$ kPa, $FS = 31.50\%$,
- Nonswelling (K)—clay with silt (siCl) [34]/clay with low plasticity (CL) [3]: $d_{10} = 0.0001$ mm, $d_{50} = 0.0046$ mm, $d_{90} = 0.05$ mm, $C_c = 1.25$, $C_u = 73$, $f_{cl} = 38\%$, $f_{si} = 60\%$, $f_{sa} = 2\%$, $PL = 20\%$, $LL = 42\%$, $\sigma_{sp} = 0$ kPa,

where: d_{10} , d_{50} , and d_{90} are equivalent diameters; C_c is the coefficient of curvature; C_u is the coefficient of uniformity; PL and LL are the Atterberg limits of plasticity and liquidity, respectively; f_{cl} , f_{si} , and f_{sa} are the content of clay, silt, and sand fractions, respectively; σ_{sp} is the swelling pressure (according to PN-EN ISO 17892-5 [35]); FS is the free-swell (according to Holtz and Gibbs (1956) [15], after Head (2006) [14]).

A detailed list of all parameters and a description of the tests from which they were obtained can be found in the works of Jastrzębska [18], Jastrzębska and Tokarz [24].

2.2 Rubber waste

One tire waste size was used in soil–rubber mixtures: granulate (G) 1–5 mm (Fig. 1). The rubber additive originated from the local shredding companies and contained negligible amounts of textile parts. The parameters characteristic for granulate (according to [24]) indicating their homogeneous nature are as follows:

- Granulate (G)– $d_{10} = 1.12$ mm, $d_{50} = 2.0$ mm, $d_{90} = 4.0$ mm, $C_c = 0.8$, $C_u = 2.1$.

The specific gravity of rubber was approximately 1.15 g/cm³, which falls within the range of values given by Akbulut et al. [2] and Kalkan [26].

2.3 Soil–rubber mixtures

For the purposes of numerical analyses, the following mixtures of pure soil (RC or K) with the addition of 0, 10, and 25% rubber waste (G) in relation to the total mass were prepared:

- RC-G-10 (90% red clay with 10% addition of granulate 1–5 mm);
- RC-G-25 (75% red clay with 25% addition of granulate 1–5 mm);
- K-G-25 (75% kaolin with 25% addition of granulate 1–5 mm);
- RC (100% red clay);
- K (100% kaolin).

The proper specimens from RC and K, and their mixtures with granulate (RC-G and K-G) were prepared by cutting the specimens directly from a block prepared in a Proctor apparatus or by pushing out from the cylindrical forms pressed into Proctor's mold (Fig. 2). A detailed description of the samples preparation was presented in the works of Jastrzębska [18], Jastrzębska and Tokarz [24]. It is worth noting that with the higher content of rubber waste, the density of soil–rubber mixtures decreased accordingly: RC – $\rho = 1.85$ g/cm³, RC-G-10 – $\rho = 1.62$ g/cm³, RC-G-25 – $\rho = 1.46$ g/cm³, K – $\rho = 1.94$ g/cm³, K-G-25 – $\rho = 1.52$ g/cm³. This fact is important in the case of loading a weak subsoil with embankments made of soil–rubber mixtures.

2.4 Triaxial test conditions

The full research program included triaxial tests: cyclic and monotonic CU (consolidated, undrained) and monotonic UU (unconsolidated, undrained) was conducted according to the Standards PN EN ISO 17892-9 [36] and PKN-CEN ISO/TS 17892-8:2009 [33], respectively. Each sample (tests CU) was saturated, initially by flushing with deaerated water, and after by using back pressure procedure (at the end of the back pressure procedure, Skempton parameter was equal to $B = 0.86$ – 0.96). The cyclic triaxial tests (CU) were carried out with a low frequency ($f \approx 0.001$ Hz, and it is low enough to exclude the presence of dynamic phenomena)



Figure 1: Rubber waste granulate (G) 1–5 mm used in triaxial tests.



Figure 2: Preparation of specimens from the red clay–granulate mixture.

and a constant stress amplitude equal to $A = 0.35q$ (where q is a deviator stress corresponding a current axial strain $\varepsilon_t = 1\%$, which corresponds to the moment when the cyclic load action started), at a constant displacement rate (controlled deformation) equal to $v_s = 0.9$ mm/h. After cyclic loading, the test was continued under a monotonic

load until an axial strain of 15% was achieved. To avoid the impact of swelling, in the case of UU triaxial tests the specimens were not saturated with deaerated water prior to shearing realized at a constant displacement rate equal to $v_s = 7.2 \text{ mm/h}$ (UU). Each series of UU tests was carried out at confining stresses equal to $\sigma_3 = 50 \text{ kPa}$, 100 kPa , and 200 kPa . Whereas each series of CU tests was conducted at confining stresses equal to $\sigma'_3 = 20 \text{ kPa}$, 50 kPa , and 80 kPa (for RC and RC-G) and $\sigma'_3 = 100 \text{ kPa}$, 200 kPa , and 300 kPa (for K-G). The selection of confining pressure $\sigma'_3 = 100 \text{ kPa}$, 200 kPa , and 300 kPa for K–rubber waste mixture tests refers to earlier Jastrzębska's tests conducted on pure K [17,19,20,21]. In turn, the choice of confining pressure $\sigma'_3 = 20 \text{ kPa}$, 50 kPa , and 80 kPa for RC–rubber waste mixture tests sought to verify whether the expansive soil (weak soil) with the addition of rubber waste could be used for road or railway embankment construction, where the real transferred loads are usually less than 100 kPa .

3 Numerical analyses

3.1 Assumptions made

Numerical analyses were performed by the finite element method using the Z_Soil 2020 program [7]. In the case of the stability analysis, a simplification was used in the form of assuming a plane strain state, which is characteristic for linear objects [5,41,44]. When analyzing the VSS plate test, the assumption of axial symmetry was adopted, which is also correct for a homogeneous substrate (at least to the depth of the test range, which is defined as $2D$, where D is the diameter of the steel rigid plate used in the test. Quadrangular, four-node finite elements were used for the analyses. In each node, the searched unknowns were the components of displacements in two directions: vertical and horizontal. A simple, elastic-perfectly plastic model with a Coulomb–Mohr yield surface was used for the analyses. Since the analysis of the single-component soil medium was limited to the analysis, the state of total stresses was analyzed, without separation into stresses taken by the soil skeleton and water in the pores. Hence, the behavior of the soil medium will be described by the integer values of the strength parameters: cohesion c_u and friction angle ϕ_u . The Coulomb–Mohr model describes the shear strength of the soil very well, hence the use of this model in stability analyses gives sufficiently accurate results [13]. The behavior of the soil medium in phase of elastic work is described by two more parameters: Young's modulus E and Poisson ratio ν .

A common problem when performing numerical analyses is the selection of parameter values used in the computation. The use of advanced constitutive models makes it necessary to specify various parameters that often do not have a simple physical interpretation, which makes it impossible to determine their values on the basis of typical laboratory or field tests. Hence, the great desire to use simple models for which it is possible to precisely determine the values of model parameters [12]. Of course, then it is necessary to perform practical verifications that will confirm the correctness of the performed numerical analyses.

3.2 Stability analysis of the embankment slopes

In the stability analysis of the slopes of the embankments, the computations were divided into two stages. The first one is the generation of the state of primary stresses, which arise from the self-weight of the soils forming the road embankment. The current state of the embankment was taken into account—the analysis of the change in the state of stress and the resulting settlements of the subsoil under the embankment during the erection of the earth structure was omitted [23]. The next step is the analysis of the stability by the strength reduction method $c-\phi$. The adopted numerical procedure assumes a gradual (in predetermined calculation steps) reduction of the cohesion value and the internal friction angle according to the following relationship (3.1) [44,47,53]:

$$F_s = \frac{c_0}{c_f} = \frac{\tan \phi_0}{\tan \phi_f}, \quad (3.1)$$

where: F_s —safety factor, which is a measure of safety due to stability; c_0, ϕ_0 —initial values of cohesion and internal friction angle; c_f, ϕ_f —values of cohesion and friction angle at the moment of completion of computation due to the lack of convergence of iterative procedures.

As a result of the decrease in the strength parameters, plastic zones, which appear in part of the model, are eliminated in subsequent iterative steps using the phenomenon of stress redistribution. The procedure is carried out until the iterative procedures do not converge, which means that the computation are completed. The results of the analyses are the value of the safety factor F_s obtained at the end of the calculations and the location of the slide surface. The abovementioned location is estimated on the basis of the analysis of the map of

total displacements at the moment of loss of stability of computation [30].

The procedure of estimating the value of the F_s factor adopted above has a great advantage compared to the so-called strip methods (Fellenius, Bishop, Janbu, Morgenstern-Price, etc.), where the user must first define the location of the slide surface [40]. In the presented method, the shape of this surface is the result of computations. The obtained stability loss mechanism corresponds to the smallest value of the safety factor (each hypothetically different failure mechanism will have a greater factor).

3.3 Simulation of the VSS test

The basic in situ test used in road construction is a load test of a rigid VSS steel plate with a diameter of 300 mm. In road jargon, it is called a test of the bearing capacity of the subsoil or road pavement structure. This test allows the assessment of the condition of the native soil layer or aggregate layer to a depth of approx. 0.5–0.6 m below the level of the steel plate base. The layers of the communication embankment are assessed in the same way, and a single test allows to visualize the condition of 1–2 layers of the embankment. The test loads are carried out in two stages. The first is the primary load, which in steps of 50 kPa reaches a value of 250–450 kPa depending on the type of the tested element (soil layer, embankment layer, lower or upper layers of the pavement structure). The next stage of the analysis is the secondary loading after unloading. In this stage, repeated pressures of approx. 100 kPa lower than in the first stage are applied. The results of the analyses are the values of the E_1 and E_2 stiffness modules obtained from the primary and secondary loading of the plate, respectively, calculated according to the formula (3.2):

$$E_1, E_2 = \frac{\Delta p}{\Delta s}, \quad (3.2)$$

where: Δp —load increment [MPa], Δs —settlement increment [mm].

In addition to the above modules, the result of the analyses is also the value of the strain ratio determined from the relationship (3.3):

$$I_0 = \frac{E_2}{E_1}. \quad (3.3)$$

When making road embankments, the requirements are $E_2 \geq 40$ MPa for the lower layers of the road embankment and $E_2 \geq 60$ MPa for layers located up to 2.0 m below the bottom base of the pavement structure [38]. In the case of the strain ratio, these requirements come down to $I_0 \leq 2.2$ for the layers located directly under the pavement structure and $I_0 \leq 2.5$ for deeper layers. The above values for the I_0 index are quite conservative. Treating the soil–rubber mixture as multigrained soils, $I_0 \leq 3.0$ would be a sufficient requirement. However, it should be pointed out that the requirements regarding the I_0 coefficient are not much justified for layers located deep under the pavement structure. Some engineers treat this value as a measure of compaction (i.e. a measure of the quality of contractors' works), however, from the point of view of soil mechanics, it is a very rough approximation having little in common with the actual properties of the corpus of the road embankment.

4 Results and discussion

4.1 Definition of numerical models

The numerical model used for the stability analysis is shown in Fig. 3. A road embankment with a height of 6 m was analyzed. Owing to the symmetry of the problem, half of the model was taken, assuming the axis of symmetry running through the center of the embankment. It should be noted that in order to be able to take into account the above simplification, the shape of the embankment, the course of layers in the subsoil, and the corpus of the embankment, as well as the assumed boundary conditions must be characterized by symmetry. The built numerical model had 2777 finite elements. Generally, the stability of a given slope is determined by the geometric shape and the strength and deformation properties of the materials that build the embankment. In the case of a weaker subsoil, the properties of the subsoil on which the embankment was erected also have a large impact on its stability. Hence, the need to take into account the subsoil to a depth that will ensure no influence of boundary conditions on the obtained analysis results. Similarly, the area of the base of the embankment should be considered. In the built model, a distance of 25 m from the base of the embankment and 20 m into the ground under the embankment was assumed. Standard geotechnical boundary conditions were used, which assume that displacements in both directions are prevented in all nodes on the lower edge of the model and horizontal displacements in nodes on both side edges are not possible. In the stability analyses, the occurrence of

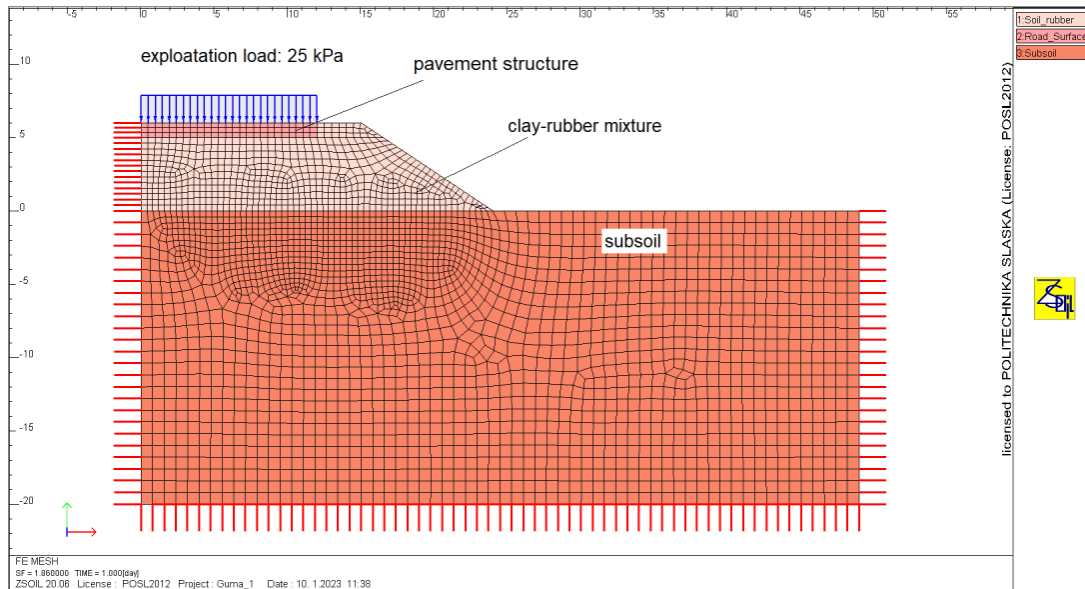


Figure 3: Model used for stability analysis

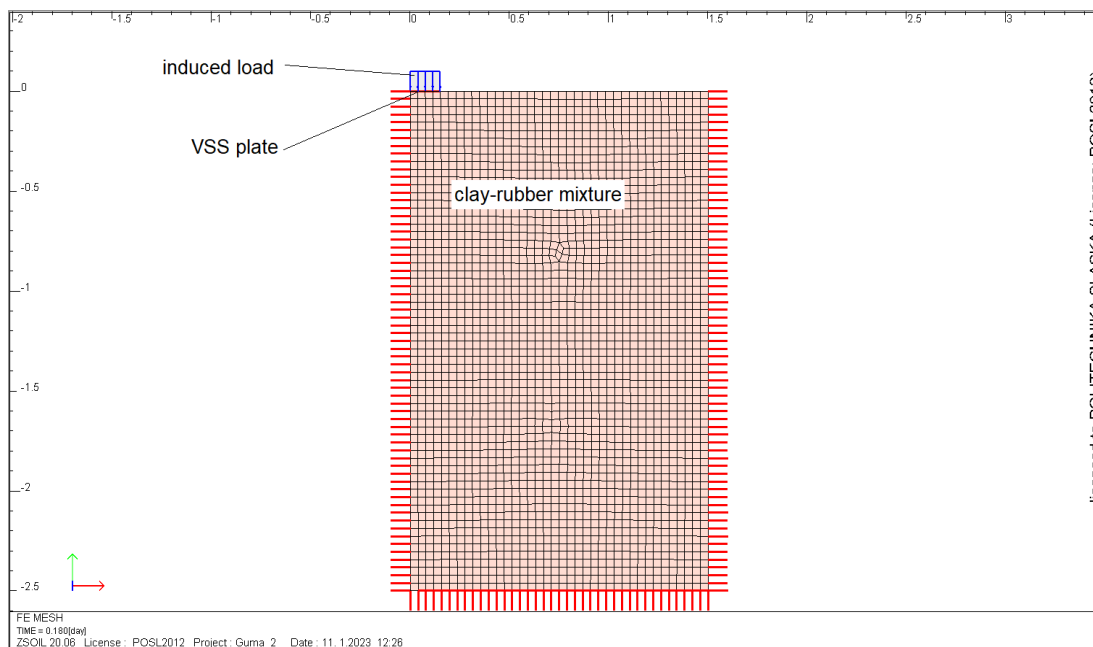


Figure 4: Model was used to analyze the properties of the subsoil under the road surface construction.

exploitation load on the road surface was additionally taken into account, which was assumed as a uniform pressure of 25 kPa exerted on the part of the embankment crown occupied by the surface structure.

With numerical analyses of VSS test load simulations, the dimensions of the geometrical model (Fig. 4) of the analyzed model are correspondingly smaller. They result from the dimensions of the plate used in the tests, the radius of which is: $D/2 = 150$ mm. The defined model has

dimensions of $5 D = 1.5$ m in the horizontal direction and $10 D = 3.0$ m in the vertical direction. These dimensions are definitely larger than those traditionally used in the analysis of foundation–soil cooperation [13]; however, in the present case, due to these dimensions, it was possible to thoroughly analyze the extent of the impact of the plate into the subsoil and determine the influence of the deeper layers on the obtained results. The number of defined finite elements in this case was 2434.

4.2 Selection of parameters for calculations

Similar to Das and Singh [9] and Tajdini et al. [46], a random change in the internal friction angle and cohesion is visible (Table 1). The results confirm the opinion that testing the soil–rubber mixture intended for engineering applications is necessary each time. Table 1 summarizes the strength parameters (internal friction angle ϕ and cohesion c) obtained from CU/UU triaxial tests. On their basis, the parameters presented in Table 2 were adopted for numerical analyses. Carefully estimated average values characterizing various cement–soil mixtures based on cyclic tests were adopted, which characterize the properties of the material under the conditions of characteristic interactions of communication structures. The parametric analysis performed in the following part will allow to assess the influence of a given parameter on the obtained results in numerical analyses. The considerate range of parameter values includes all the values obtained in tests for the analyzed materials.

A total of 3 material zones were adopted. When analyzing the stability of the embankment slopes, the parameters of the elements simulating the behavior of the layers of the pavement structure, as well as the elements being the subsoil, were adopted in such a way that these layers did not affect the obtained analysis results. Therefore, the situation when the slope stability is affected by a weak subsoil was not analyzed. The problem defined in this way will allow to assess the possibility of using the tested material in road construction.

The most important, from the point of view of the issues discussed in the article, are the parameters of the soil–rubber mixture from which the embankment was made. These values were estimated based on mean values obtained in laboratory tests (Table 1, [18,24]). A careful estimation of the parameter values was adopted, which allows us to treat them as derived values (experts) according to the Eurocode 7 standard. The properties of the subsoil under the embankment were assumed in such a way that the subgrade did not determine the obtained results. The results of numerical analyses will make it possible to assess the possibility of using the tested material in road construction from the point of view of the strength and deformation properties and the impact of these properties on the results of acceptance tests, as well as the safety margin due to the stability of the embankment.

Table 1: The strength parameters obtained from CU/UU triaxial tests.

Type of material	CU triaxial tests (cyclic/(*) monotonic)		CU triaxial tests (monotonic)	
	Internal friction angle ϕ [°]	Cohesion c [kPa]	Internal friction angle ϕ [°]	Cohesion c [kPa]
RC-G-10	24	61	24	62
RC-G-25	15	30	28	22
K-G-25	9	70	–	–
RC	–	–	21	167
K	25*	11*	–	–

Table 2: Parameters taken for numerical analyses.

Material zone	Volumetric weight [kN/m ³]	Cohesion c [kPa]	Internal friction angle ϕ [°]	Stiffness modulus E [MPa]
The corpus of the embankment (soil–rubber mixture)	15.0	30	15	60
Subsoil under the embankment	21.0	5	30	40
Pavement structure	22.0	Elastic material		800

4.3 Course of analyses

The analysis of the slope stability of the road embankment was carried out in three stages. The first one is the generation of the state of primary stresses in the subsoil and the corpus of the embankment, which results from the self-weight of the soils and materials. Next, the operational load of the road surface was set in calculation steps. The third and most important stage was the stability analysis carried out using the c – ϕ strength reduction method, which was described earlier. After the computations are completed, which takes place when the numerical procedures do not converge, it is possible to estimate the location of the slip surface corresponding to the lowest value of the safety factor F_s .

The first stage of the numerical simulation of VSS plate load test tests is also the generation of the primary stress state. Owing to the dimensions of the model, in this case the obtained values are definitely smaller. Next, the load transferred to the steel plate was applied. The path of the primary load was carried out, obtaining the value of 350 kPa. Next the unloading and reloading process to the value of 250 kPa was realized. The obtained values of

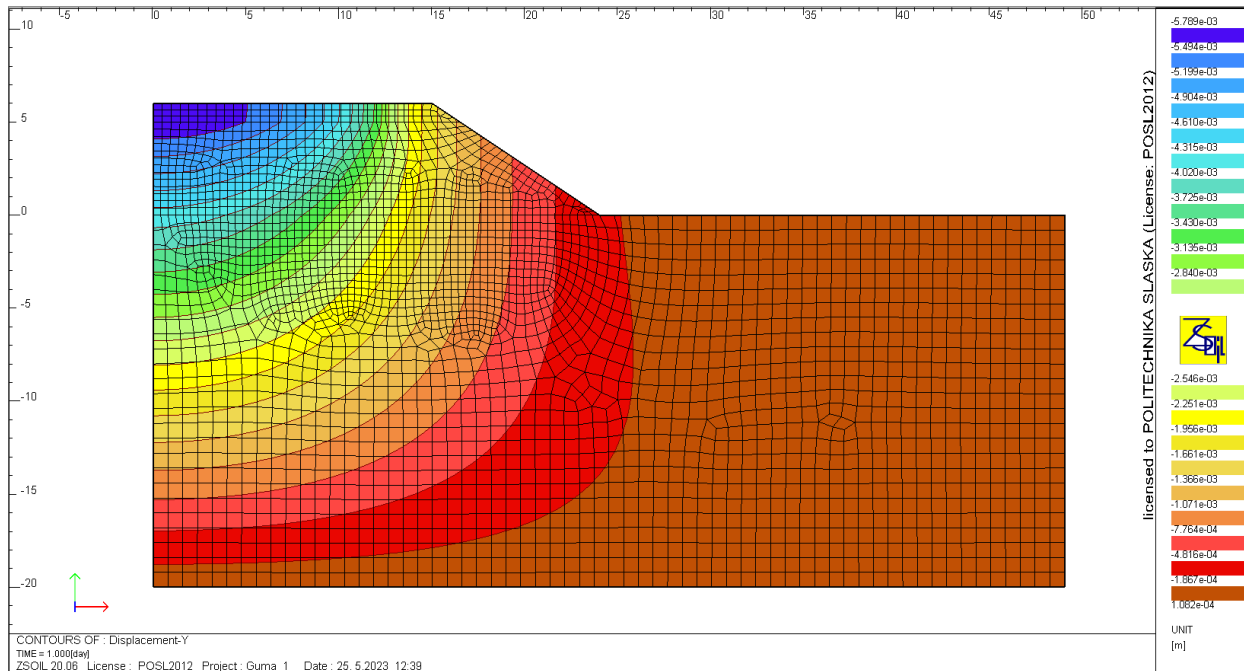


Figure 5: Settlements caused by the exploitation load of the road surface.

displacements of the plate center will allow to calculate the values of modules E_1 and E_2 and the strain ratio I_0 .

4.4 Results obtained from the numerical analyses

The results of analyses of the behavior of the road embankment erected with using the analyzed rubber–soil material are presented in Figures 5–9. The first of them (Fig. 5) shows the values of settlements due to operational loads of the road surface structure. The maximum settlement amounts to 5.8 mm and these values are within the requirements of the relevant regulations and standards [37,38,39]. Fig. 6 shows the yield surface at the moment of loss of stability, which corresponds to the value of the safety factor $F_s = 2.26$. This area can be estimated on the basis of the map of total displacements. The yield surface corresponds to the sliding of earth masses along the cylindrical surface running through the corpus of the embankment. Attention should be paid to the very high value of the F_s coefficient, which results from the high strength parameters of the analyzed rubber–soil material.

As part of the numerical analyses performed, the impact of the cohesion and the internal friction angle values on the value of the safety factor was also carried out. The results of these analyses are presented in the figures below. It is easy to see that the cohesion is the decisive

factor in the safety margin (Fig. 7a). If a sufficiently high value of cohesion is confirmed, this material will be an excellent component that will guarantee safe use of the communication structure. It is also easy to notice the large influence of the value of the internal friction angle (Fig. 7b).

The results of the second of the performed analyses—simulation of the VSS plate test, on the basis of which the properties of the subsoil and embankment layers in road construction are determined, are shown in Fig. 8. Based on the stress–settlement relationship, from the appropriate load phases, the values of the stiffness modulus and the strain ratio can be determined. The obtained modules for the results presented in the Fig. 8 are equal to: $E_1 = 24.2$ MPa, $E_2 = 56.7$ MPa and $I_0 = 2.35$. They have been calculated for the appropriate ranges of stresses related to the subsoil. These results meet the requirements for the subsoil or even lower layers of the road embankment on which the road surface structure will be made (30–40 MPa—depending on the road class). To be able to use the material to make layers with higher requirements, it would have to have a higher value of Young’s modulus, which is a measure of material stiffness. An important result is also the settlement map (Fig. 9), which indicates the depth of the impact of the load transmitted by the VSS plate into the subgrade. Based on this observation, it can be concluded that it is necessary to test each layer of the formed embankment, while the study of the native subsoil

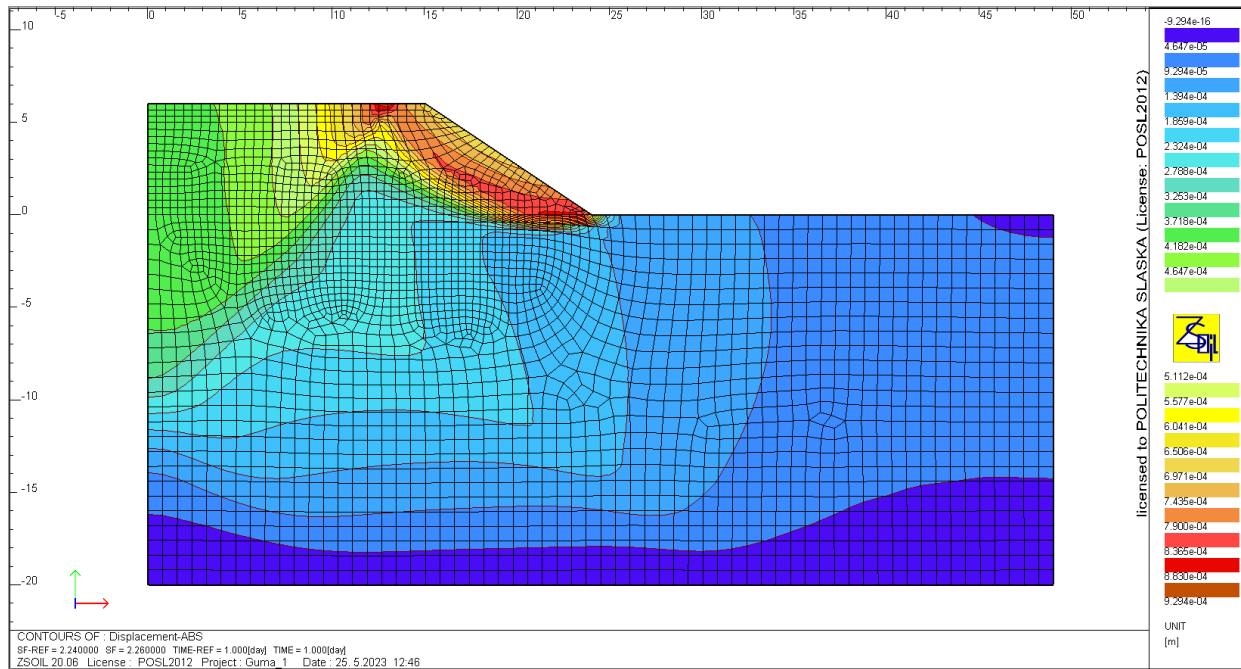


Figure 6: Map of total displacements at the moment of loss of stability of the embankment slope.

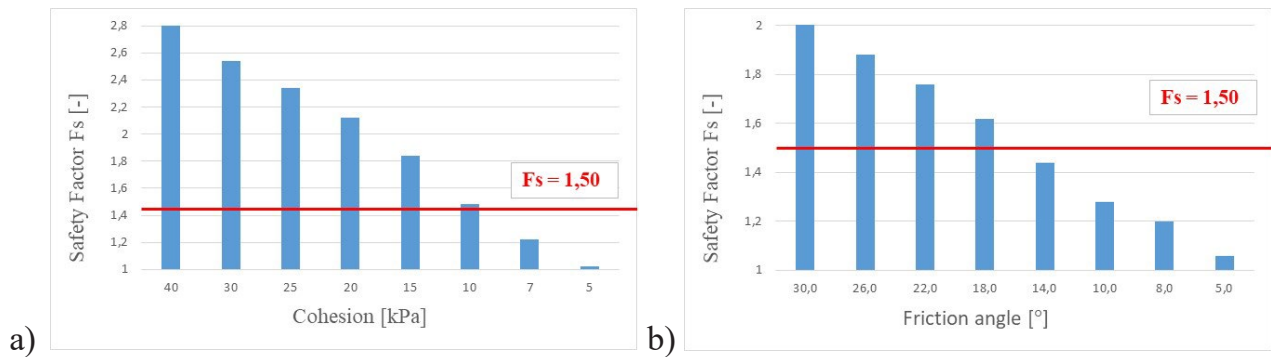


Figure 7: Analysis of the impact of strength parameters on the value of the safety factor: a) cohesion, b) internal friction angle.

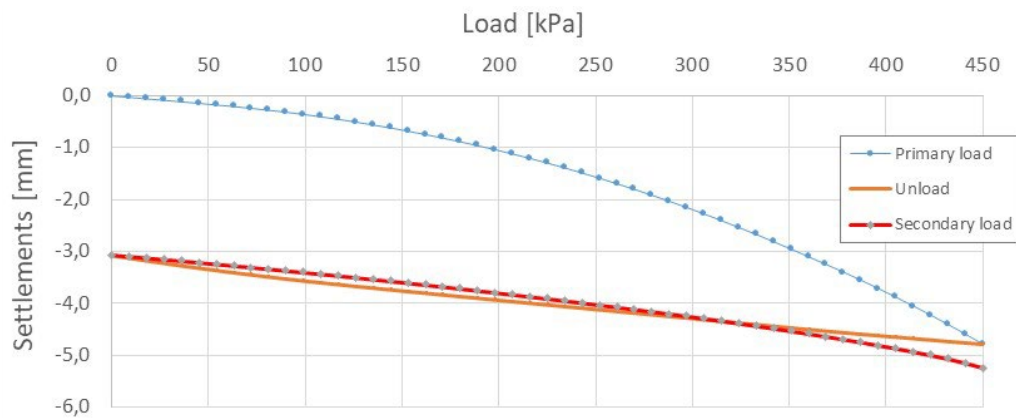


Figure 8: Stress-settlement relationship for the VSS plate load test simulation.

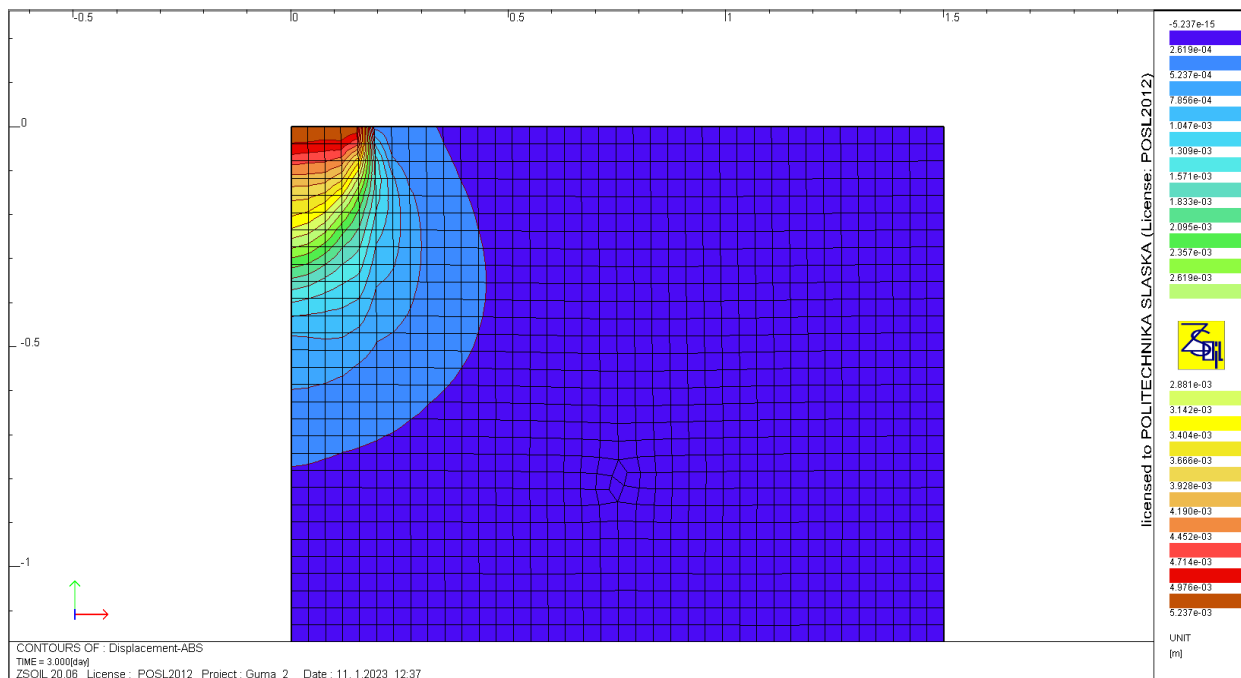


Figure 9: Map of settlements caused by the load transmitted by the VSS plate.

gives information about their deformation properties only to a small depth.

5 Conclusions

Based on the considerations carried out, it can be concluded that the numerical model of the analyzed issues presented in this article is the right tool for assessing the properties of objects made from the analyzed material.

The results obtained in the performed numerical analyses indicate that the soil–rubber material, provided that appropriate properties are obtained in laboratory and field tests, can be used in the corpus of communication embankments, as well as in the lower layers of the pavement structure. Very favorable values of cohesion and internal friction angle guarantee obtaining the appropriate stability coefficient, as well as the required results in VSS plate tests, which are the basic tests carried out during road works. In cases of practical use of this type of materials in road construction, numerical analyzes must be preceded by the proper determination of model parameters in laboratory tests.

The results of laboratory tests confirm the necessity of testing soil–rubber mixtures each time before their use in embankments. The observed overall decrease in shear strength and stiffness of the tested material is variable

and depends on the type of soil and the content of rubber waste. In some cases, an addition of 5% granulate is more preferable, and in other situations—10%. However, this recommended addition of granulate should not exceed 30% by weight.

An important element of the designing process with the use of soil–rubber mixtures is the performance of numerical analyses, which, based on the results of laboratory tests, will allow to estimate the properties of the obtained layers. In particular, a simulation of the VSS slab load test should be carried out, which is crucial in the implementation of road construction works. In addition, it is extremely important to perform slope stability analyses, especially in the case of high embankments. Stability of slopes is largely determined by the strength properties of the lower layers of embankments, hence numerical analyses allow for realistic estimation of the existing safety margin.

Performed numerical analyses showed that the addition of rubber granulate in the amount of 5–25% allows the use of the material (depending on the road class) for road embankments or lower layers of the pavement structure.

References

- [1] Akbarimehr, D., Aflaki, E. (2018). An Experimental Study on the Effect of Tire Powder on the Geotechnical Properties of Clay Soils. *Civ. Eng. J.*, 4, 594.
- [2] Akbulut, S., Arasan, S. and Kalkan, E. (2007). Modification of Clayey Soils using Scrap Tire Rubber and Synthetic Fibers. *Appl. Clay Sci.*, 38, pp. 23–32.
- [3] ASTM D2487-11 (2017). In Standard Practice for Classification of Soils for Engineering Purposes (Unified Soil Classification System); ASTM International: Philadelphia, PA, USA.
- [4] Batog, A., Stilger-Szydło, E. (2018). Stability of road earth structures in the complex and complicated ground conditions. *Studia Geotechnica et Mechanica*, 40(4).
- [5] Cała, M. (2007). Convex and concave slope stability analyses with numerical methods. *Archives of Mining Science*, 52(1), pp. 75–89.
- [6] Cetin, H., Fener, M. and Gunaydin, O. (2006). Geotechnical Properties of Tire-Cohesive Clayey Soil Mixtures as a Fill Material. *Eng. Geol.*, 88, pp. 110–120.
- [7] Commend, S., Kivell, S., Obrzud, R., Podleś, K. and Truty, A. (2020). Computational Geomechanics & Applications with ZSOIL.PC. Lausanne: Zace Services Ltd, Software Engineering, 2020.
- [8] Das, C., Ghosh, A. (2020). Study on River Bed Material and Numerical Analysis of Stabilized Road Embankment on Soft Soil. In: Prashant, A., Sachan, A., Desai, C. (eds) *Advances in Computer Methods and Geomechanics. Lecture Notes in Civil Engineering*, vol 55. Springer, Singapore.
- [9] Das, T., Singh, B. (2012). Strength Behaviour of Cohesive Soil-Fly Ash-Waste Tyre Mixtures. In *Proceedings of the SAIMT Research Symposium on Engineering Advancements*, University of Moratuwa, Malabe, Sri Lanka, 27–28 April 2012, pp. 35–38.
- [10] Gomes Correia, A., Winter, M.G. and Puppala, A.J. (2016). A review of sustainable approaches in transport infrastructure geotechnics. *Transportation Geotechnics*, 7, pp. 21–28.
- [11] Griffiths, D.V., Lane, P.A. (1999). Slope stability analysis by finite elements, *Geotechnique*, 49, pp. 387–403.
- [12] Gryczmański, M. (1995). Introduction to the description of elastic-plastic soil models. *Committee of Civil and Water Engineering of the Polish Academy of Sciences*, no 40, Warszawa. (in Polish)
- [13] Gryczmański, M. (2009). State of the art in modelling of soil behaviour at small strains, *ACEE Archit. Civ. Eng. Environ.*, 2(1), pp. 61–80.
- [14] Head, K.H. (2006). *Manual of Soil Laboratory Testing: Soil Classification and Compaction Test*, 3rd ed.; Whittles Publishing: Scotland, UK, Volume 1.
- [15] Holtz, W.G.; Gibbs, H.J. (1956). Engineering Properties of Expansive Clays. *Trans. Am. Soc. Civ. Eng.*, 121, 641–663.
- [16] Indraratna, B., Rujikiatkarnjorn, C., Tawak, M. and Heitor, A. (2019). Compaction, Degradation and Deformation Characteristics of an Energy Absorbing Matrix. *Transp. Geotech.*, 19, pp. 74–83.
- [17] Jastrzębska, M. (2010). Investigations of the Behaviour of Cohesive Soils Subject to Cyclic Loads in the Area of Small Deformations, Monograph, D.S., Ed., Silesian University of Technology Publishers: Gliwice, Poland.
- [18] Jastrzębska, M. (2019). Strength Characteristics of Clay-Rubber Waste Mixtures in UU Triaxial Tests. *Geosciences*, 9(8):352.
- [19] Jastrzębska, M. (2010). The External and Internal Measurement Impact on Shear Modulus Distribution within Cyclic Small Strains in Triaxial Studies into Cohesive Soil. In *Proceedings of the EPJ Web of Conferences*, Poitiers, France, 10 June 2010, Volume 6, p. 22014.
- [20] Jastrzębska, M. (2010). The Influence of Overconsolidation Ratio on the “ G_s - ϵ_1 ” Dependence for Cyclic Loading of Cohesive Soils in the Range of Small Strains. *Studia Geotechnica et Mechanica*, 32, pp. 17–28.
- [21] Jastrzębska, M. (2010). The Influence of Selected Parameters of Cyclic Process on Cohesive Soils Shear Characteristics at Small Strains. *Arch. Civ. Eng.*, 56, pp. 89–107.
- [22] Jastrzębska, M., Kazimierowicz-Frankowska, K., Chiaro, G. and Rybak, J. (2023). New Frontiers in Sustainable Geotechnics. *Applied Sciences*, 13(1):562.
- [23] Jastrzębska, M., Łupieżowiec, M. (2018). Analysis of the causes and effects of landslides in the Carpathian Flysch in the area of Miłówka commune and evaluation of the methods of their prevention, *Annal. Warsaw Univ. Life Sci. – SGGW, Land Reclamation*, 50(2), pp. 195–211.
- [24] Jastrzębska, M., Tokarz, K. (2021). Strength Characteristics of Clay-Rubber Waste Mixtures in Low-Frequency Cyclic Triaxial Tests. *Minerals*, 2021, 11(3):315.
- [25] Kalantari, B. (2012). Foundations on Expansive Soils: A Review. *Res. J. Appl. Sci. Eng. Technol.*, 4, pp. 3231–3237.
- [26] Kalkan, E. (2013). Preparation of Scrap Tire Rubber Fiber-Silica Fume Mixtures for Modification of Clayey Soils. *Appl. Clay Sci.*, 80–81, pp. 117–125.
- [27] Kliszczewicz, B., Kowalska, M. (2020). Numerical Study of the Use of Tyre-Derived-Aggregate (TDA) as the Backfill Above Flexible PVC Pipeline. In *Proceedings of the IOP Conference Series: Materials Science and Engineering*, Prague, Czech Republic, 15–19 June 2020, Vol. 960, pp. 32–44.
- [28] Kowalska, M., Chmielewski, M. (2017). Mechanical Parameters of Rubber-Sand Mixtures for Numerical Analysis of a Road Embankment. In *Proceedings of the IOP Conference Series, Materials Science and Engineering*, Beijing, China, 24–27 October 2017, Vol. 245:052003.
- [29] Kowalska, M., Jastrzębska, M. (2017). Swelling of Cohesive Soil with Rubber Granulate. In: *Analizy i Doświadczenia w Geoinżynierii*, Bzówka, J., Łupieżowiec, M., Eds., Politechnika Śląska: Gliwice, Poland, Vol. 651, pp. 261–270.
- [30] Łupieżowiec, M. (2013). The application of c - ϕ reduction method to estimate the bearing capacity of subsoil. *ACEE Architecture Civil Engineering Environment*, 6(4), pp. 35–43.
- [31] Łupieżowiec, M., Rybak, J., Różański, Z., Dobrzycki, P., Jędrzejczyk, W. (2022). Design and Construction of Foundations for Industrial Facilities in the Areas of Former Post-Mining Waste Dumps. *Energies*, 15(16).
- [32] Mickovski, S.B. (2021). Sustainable Geotechnics – Theory, Practice, and Applications. *Sustainability*, 13(9):5286.
- [33] PKN-CEN ISO/TS 17892-8:2009 (2009). In *Geotechnical Investigation and Testing – Laboratory Testing of Soil – Part 8: Unconsolidated Undrained Triaxial Test*, PKN: Warszawa, Poland.
- [34] PN-EN ISO 14688-2:2006 (2006). In *Geotechnical Investigation and Testing – Determination and Classification of Soils – Part 2: Classification Rules*, PKN: Warszawa, Poland.

- [35] PN-EN ISO 17892-5:2017-06 (2017). In Geotechnical Investigation and Testing – Laboratory Testing of Soil – Part 5: Incremental Loading Oedometer Test; PKN: Warszawa, Poland.
- [36] PN-EN ISO 17892-9:2018-05 (2020). In Geotechnical Investigation and Testing – Laboratory Testing of Soil – Part 9: Consolidated Triaxial Compression Test on Water Saturated, PKN: Warszawa, Poland.
- [37] PN-EN 1997-1:2008 (Eurocode 7) (2008). Geotechnical design – Part 1: General principles. PKN: Warszawa, Poland.
- [38] PN-S-02205:1998 (1998). Car roads, Spadeworks, Research and Requirements. PKN: Warszawa, Poland.
- [39] Regulation (1999). Regulation of the Minister of Transport and Maritime Economy of March 2, 1999 on the technical conditions to be met by public roads and their location, Journal of Laws of 2016, pos. 124. (in Polish)
- [40] Salunkhe, D.P., Bartakke, R.N., Chvan, G., Kothavale, P.R. and Digvijay P. (2017). An overview on methods for slope stability analysis. *International Journal of Engineering Research & Technology (IJERT)*, 6(3), pp. 528–535.
- [41] Sloan, S.W. (2013). Geotechnical stability analysis. *Geotechnique*, 63(7), pp. 531–571.
- [42] Soltani, A., Deng, A., Taheri, A., Mirzababaei, M. and Vanapalli, S.K. (2019). Deng Swell–Shrink Behavior of Rubberized Expansive Clays During Alternate Wetting and Drying. *Minerals*, 9, 224.
- [43] Soltani, A., Deng, A., Taheri, A. and Sridharan, A. (2019). Swell–Shrink–Consolidation Behavior of Rubber–Reinforced Expansive Soils. *Geotech. Test. J.*, 42, pp. 761–788.
- [44] Ślusarek, J., tupieżowiec, M. (2020). Analysis of the influence of soil moisture on the stability of a building based on a slope. *Engineering Failure Analyses*, 113:104534.
- [45] Tafti, M.F., Emadi, M.Z. (2016). Impact of Using Recycled Tire Fibers on the Mechanical Properties of Clayey and Sandy Soils. *Electron. J. Geotech. Eng.*, 21, pp.7113–7125.
- [46] Tajdini, M., Nabizadeh, A., Taherkhani, H. and Zartaj, H. (2016). Effect of Added Waste Rubber on the Properties and Failure Mode of Kaolinite Clay. *Int. J. Civ. Eng.*, 15, pp. 949–958.
- [47] Urbański, A., Grodecki, M. (2019). Protection of a building against landslide. A case study and FEM simulations. *Bulletin of the Polish Academy of Sciences-Technical Sciences*, 67(3), pp. 657–664.
- [48] Wasił, M., Zabielska-Adamska, K. (2022). Tensile Strength of Class F Fly Ash and Fly Ash with Bentonite Addition as a Material for Earth Structures. *Materials*, 15(8):2887.
- [49] Wysokiński, L. (2011). Evaluation of the stability of slopes and slopes. Security selection rules - instruction. Warszawa. (in Polish)
- [50] Yadav, J.S., Tiwari, S.K. (2019). The Impact of End-of-Life Tires on the Mechanical Properties of Fine-Grained Soil: A Review. *Environ. Dev. Sustain.*, 21, pp. 485–568.
- [51] Zabielska-Adamska, K. (2020). Sewage Sludge Bottom Ash Characteristics and Potential Application in Road Embankment. *Sustainability*, 12(1):39.
- [52] Zabielska-Adamska, K., Dobrzycki, P. and Wasił, M. (2023). Estimation of Stiffness of Non-Cohesive Soil in Natural State and Improved by Fiber and/or Cement Addition under Different Load Conditions. *Materials*, 16(1):417.
- [53] Zheng, Y., Tang, X., Zhao, S., Deng, C. and Lei, W. (2009). Strength reduction and step-loading finite element approaches in geotechnical engineering, *J. Rock Mech. Geotech. Eng.*, 1(1), pp. 21–30.